Design of Integrated Magnetic Transformer for ZVS Phase Shift Full Bridge Converter

Xin-Lan Li*, Eun-Sung Jang*, Yong-Whan Shin*, Jae-Sun Won**, Jong-Sun Kim**, Dong-Seong Oh**, Hwi-Beom Shin*

*Dept. of Electrical Engineering, Gyeongsang National University
** Samsung Electro-mechanics Co. Ltd.

Abstract

This integrated magnetic (IM) transformer is proposed for a phase shifted full bridge (PSFB) converter with zero voltage switching (ZVS). In a new IM transformer, the transformer is located on the center leg of E-core and the output inductor is wound on two outer legs. The proposed circuit is analyzed electrically and magnetically. An E-core is redesigned and implemented. The proposed IM transformer is experimentally compared with the conventional one through a 1.2kW prototype converter.

1. Introduction

The IM transformers begin to be used in the low output voltage and high current power electronics system [1]. With the IM technique, two or more magnetic components are integrated in one magnetic structure. The EE or EI core is commonly utilized. The magnetic parts in the converter may be reduced, so that the size and power density can be improved. In some case, overall efficiency may be increased and an EMI problem may be reduced.

For a PSFB converter, several IM transformers are proposed [2]. The transformer winding is typically located on the two outer legs in series connection and the inductor is wound on the center leg. The AC flux of transformer and a half of the DC flux of inductor flows in outer legs but the inductor flux only flows in the center leg. The flux density in outer legs is much higher than one in center leg because the center leg has nearly two time cross-sectional area of the outer leg. This IM transformer has a high magnetizing inductance. Since the transformer coupling is low, EMI may be high.

A new IM transformer is proposed for ZVS PSFB converter in this paper. The transformer winding is located on the center leg for close magnetic coupling and the inductor is wound on two outer legs in series connection. The proposed IM transformer is analyzed electrically and magnetically. An E-core is redesigned and implemented. The proposed IM transformer is experimentally compared with the conventional one through a 1.2kW prototype ZVS PSFB converter and the performance is discussed.

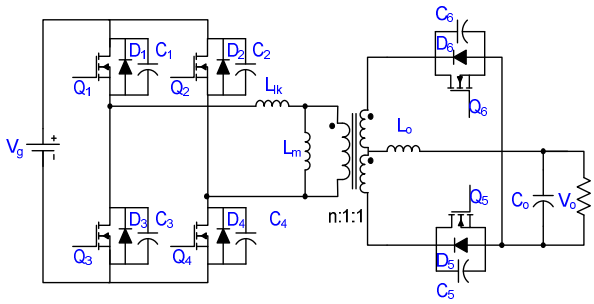

Fig. 1 ZVS PSFB converter.

2. ZVS PSFB converter and IM transformer

The ZVS PSFB converter is shown in Fig. 1. The center-tapped transformer and the output inductor are usually integrated in one EE or EI core. Fig. 2(a) shows the proposed IM transformer and the circuit connection in the output stage. The transformer and output inductor are located on the center leg and two outer legs, respectively. The conventional IM transformer given in [2] is shown in Fig. 2(b).

When the PSFB converter operates in ZVS, there are 8 operating modes during each cycle as shown in Fig. 3. The ZVS transition intervals are magnified in Fig. 3 and these intervals can be neglected when analyzing the magnetic circuit. Hence, 4 modes only are considered for analysis. The duty ratio D is limited below 0.5 because of the alternating current.

The magnetic states within each core leg are modeled by using the capacitive modeling method [3]. For simplicity, all the devices are assumed to be ideal. The permeance of core is assumed to be infinite. The operation is explained as follows.

Mode 1: $0 < t < DT_S$

In Fig. 1, both Q1 and Q4 are ON. The mode is shown in Fig. 4(a). The primary voltage V_p is positive and the secondary current flows through N_{s1}, N_L, D_5, and the load. From Fig. 4(a), the following equations can be obtained as

$$\dot{\Phi}_c = \frac{V_g}{N_p} \tag{1}$$

$$\dot{\Phi}_1 = \frac{1}{2}\left\{(1 + N_s / N_L)\frac{V_g}{N_p} - \frac{V_0}{N_L}\right\} \tag{2}$$

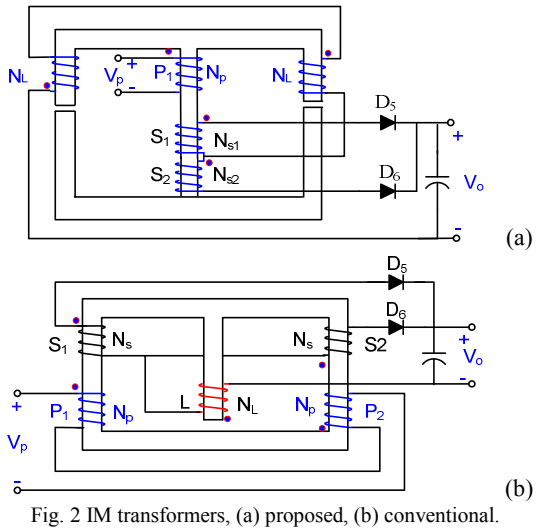

Fig. 2 IM transformers, (a) proposed, (b) conventional.

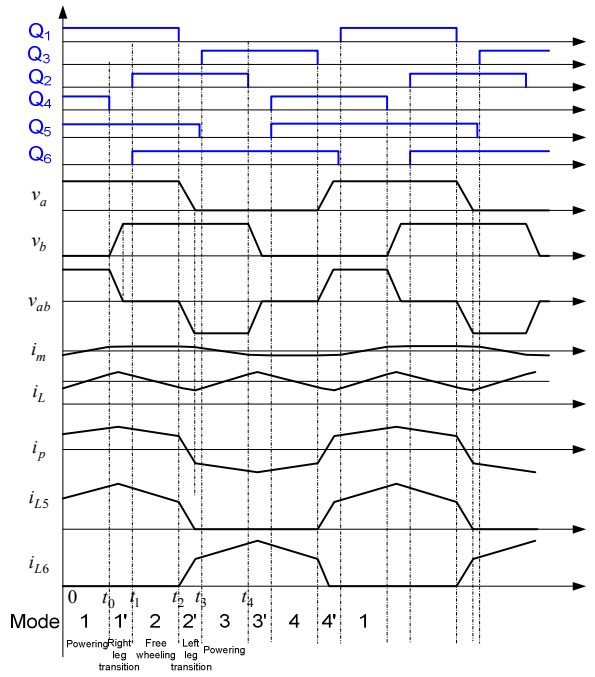

Fig. 3 Operational waveforms.

$$\dot{\Phi}_2 = \frac{1}{2}\left\{(1 - N_s / N_L)\frac{V_g}{N_p} + \frac{V_0}{N_L}\right\} \tag{3}$$

where

$\dot{\Phi}_c$: flux rate of center leg $\dot{\Phi}_1$: flux rate of right leg

$\dot{\Phi}_2$: flux rate of left leg N_p: primary winding turns

N_s: secondary winding turns N_L: inductor winding turns

V_g : input voltage V_0 : output voltage

The flux in center leg increases. The fluxes in outer legs may increase or decrease depending on the numbers of winding turns.

Mode 2: $DT_S < t < 0.5T_S$

In this mode, both Q1 and Q2 are ON as shown in Fig.3. The primary winding is freewheeling and the primary voltage is zero. The diode D_5 keeps conducting the inductor current. Mode 2 is similar to Mode 1 except the value of primary voltage. From Fig. 4(a) the flux rate in each leg can be expressed as

$$\dot{\Phi}_c = 0 \tag{4}$$

$$\dot{\Phi}_1 = -\frac{V_0}{2N_L} \tag{5}$$

$$\dot{\Phi}_2 = \frac{V_0}{2N_L}. \tag{6}$$

The flux in center leg keeps constant. The flux in left leg decreases and the flux in right leg increases.

Mode 3: $0.5T_S < t < (0.5 + D)T_S$

Both Q2 and Q3 are ON as shown in Fig.3. During Mode 3, the primary voltage V_p is negative and the secondary current flows through N_{s2}, N_L, D_6, and the load. From Fig. 4(b), the following equations can be derived as

$$\dot{\Phi}_c = -\frac{V_g}{N_p} \tag{7}$$

$$\dot{\Phi}_1 = -\frac{1}{2}\left\{(1 - N_s / N_L)\frac{V_g}{N_p} + \frac{V_0}{N_L}\right\} \tag{8}$$

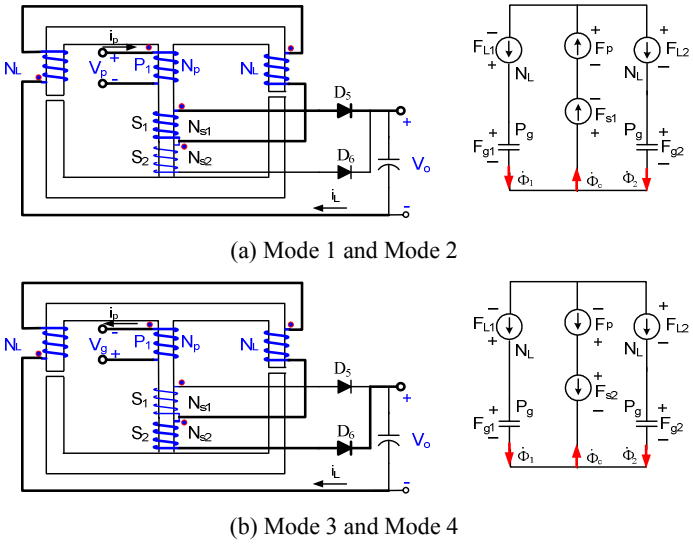

(a) Mode 1 and Mode 2

(b) Mode 3 and Mode 4

Fig. 4 Operational modes and capacitor models of proposed IM transformer.

$$\dot{\Phi}_2 = -\frac{1}{2}\left\{(1 + N_s / N_L)\frac{V_g}{N_p} - \frac{V_0}{N_L}\right\} \tag{9}$$

The flux in center leg decreases. The fluxes in outer legs may increase or decrease depending on the numbers of winding turns.

Mode 4: $(0.5 + D)T_S < t < T_S$

In this mode, both Q3 and Q4 are ON and there is no power transfer from primary side to secondary side. The diode D_6 keeps conducting the inductor current. the primary current increase. From Fig.4 (b) the flux rates are same as in Mode 2 as

$$\dot{\Phi}_c = 0 \tag{10}$$

$$\dot{\Phi}_1 = -\frac{V_0}{2N_L} \tag{11}$$

$$\dot{\Phi}_2 = \frac{V_0}{2N_L}. \tag{12}$$

Fig. 5 shows magnetic waveforms by using (1) ~ (12). The inductor in the outer legs should have a DC flux level stored in the air gap but the transformer winding in the center leg has only AC flux. The average flux rate of the inductor winding should be zero during a PWM interval. The voltage conversion ratio can then be derived, by averaging the flux rate in one inductor winding as

$$M(D) = \frac{V_0}{V_g} = 2D\frac{N_s}{N_p}. \tag{13}$$

The inductance of output inductor can be derived from Fig. 2(a) as

$$L_0 = 2N_L{}^2 P_g. \tag{14}$$

P_g denotes the air gap permeance in a outer leg and is given by

$$P_g = \frac{\mu_0 A_0}{l_g} \tag{15}$$

where μ_0 is permeability of air. A_0 and l_g are the cross-sectional area of outer leg and air gap length, respectively. The magnetizing inductance at the primary side can be found from Fig. 2(a) as

$$L_m = 2N_p{}^2 P_g. \tag{16}$$

The peak-to-peak ripple and peak flux in the outer leg are

$$\Delta\Phi_{outer\_leg} = \frac{V_0}{4f_s}\left(\frac{1}{N_s} + \frac{1+2D}{N_L}\right) \tag{18}$$

$$\Phi_{outer\_leg\_peak} = N_L P_g I_L + \frac{1}{2}\frac{V_0}{4f_s}\left(\frac{1}{N_s} + \frac{1+2D}{N_L}\right). \tag{19}$$

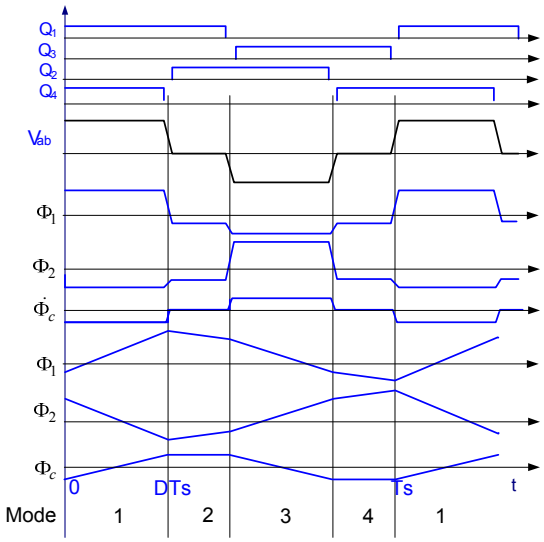

Fig. 5 Magnetic waveforms of the proposed IM transformer.

The peak-to-peak ripple flux and peak flux in the center leg are

$$\Delta\Phi_{center\_leg} = \frac{V_0}{2 f_s N_s} \quad (20)$$

$$\Phi_{center\_leg\_peak} = \frac{V_0}{4 f_s N_s} . \quad (21)$$

3. Experimental results

A 100 kHz, 1.2 kW/12 V full bridge dc-dc prototype module is designed and built to verify the proposed IM transformer. The design specifications are given in Table I.

For transformer turns ratio 20:1, the duty ratio D=0.3 for normal condition. The number of turns of each winding is chosen as

$$N_p = 40 \qquad N_{s1} = N_{s2} = 2 \qquad N_L = 2 .$$

Fig. 6 shows external appearance of the proposed IM (length×width×height: 52.1×38.0×29.2 mm) and the conventional IM (length×width× height: 64.8×37.1×30.8 mm). An E-core is redesigned such that the cross-sectional area of center leg equals to that of the outer leg. In the commercial E-core, the center leg area is about 2 times the outer leg area. The core material is PL-9. With the newly designed core, the volume can be reduced and the power density can be expected to be increased. In the proposed IM transformer, the magnetizing inductance is 462.17 μH, leakage inductance is 5.12 μH, and the output inductance is 1.33 μH.

Fig. 7 compares the electrical waveforms for the proposed and conventional IM transformers. Since the magnetic path of the proposed IM transformer has an air gap, the magnetizing inductance will be lower. Thus a peak current of primary winding increases but the effect of magnetizing inductance is less significant when the load increases.

Fig.8 shows the experimental efficiency comparison. When the load is low, the efficiency of conventional IM is high and the proposed IM efficiency increases with increasing load. At full load, similar efficiency is obtained.

Table I Circuit specifications

Rated output power	1.2 kW
Input voltage	350 ~ 410 Vdc
Output voltage	12 Vdc
Switching frequency	100 kHz
Output inductance	0.656 μH
Turns ratio of transformer	20:1
Maximal flux density	0.2 T

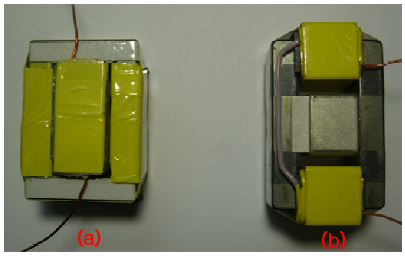

Fig.6 External appearance (a) proposed (b) conventional.

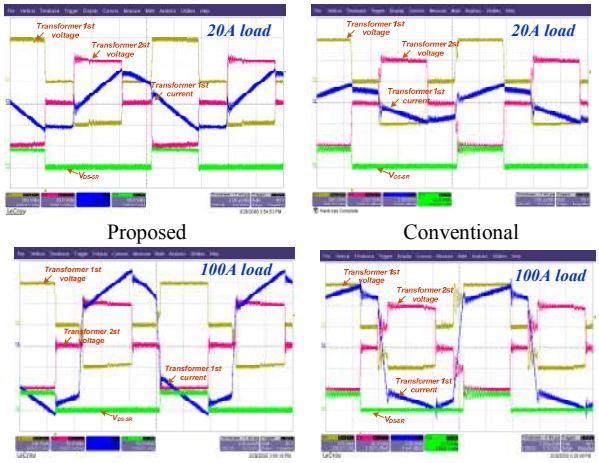

Fig. 7 Experiment results, (a) 20A load, (b) 100A load.

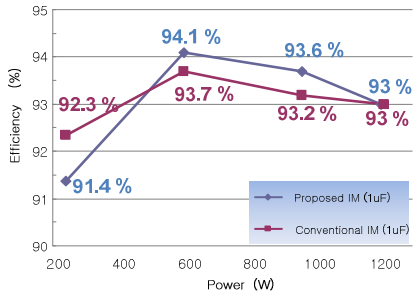

Fig. 8 Efficiency comparison.

4. Conclusion

A new integrated magnetic transformer for ZVS phase shift full bridge converter is presented. In the case of the proposed IM, DC/DC converter efficiency about 93 % is obtained at full load. The transformer size is smaller than conventional IM so that the power density increases and EMI can be reduced. The proposed IM transformer can be applied to other high frequency converter.

Acknowledgment

The paper is financially supported by Samsung Electro-mechanics Co. Ltd.

References

[1] P. Xu, Q. Wu, P. L. Wong, and F. C. Lee, "A novel integrated current doubler rectifier," in *Proc. IEEE APEC'00*, vol.2, pp.735-740, Feb. 2000.

[2] L. Yan, D. Qu, and B. Lehman, "Integrated magnetic full wave converter with flexible output inductor," *IEEE Trans. Power Electron*., vol.18, pp.670-678, Mar. 2003.

[3] D. C. Hamill, "Gyrator-capacitor modeling: a better way of understanding magnetic components," in *Proc. IEEE APEC'94*, vol.1, pp.326-332, Feb. 1994.